Automated Coding of Sewer CCTV Faults and Features

J. Myrans[1]*, R. Everson[1], Z. Kapelan[1,2] & R. Danilovic[3]

[1] University of Exeter, Harrison Building, North Park Road, Exeter, Devon, UK, EX4 4QF

[2] TU Delft, Building 23, Stevinweg 1, 2628, CN, Delft, Netherlands

[3] South West Water, Peninsula House, Rydon Lane, Exeter, Devon, UK, EX2 7HR

*Corresponding author email: j.myrans@exeter.ac.uk

Highlights

- The method identifies a specific fault code in a sewer CCTV image from a list of 102 available codes
- A CCTV image known to contain a specific fault type can be coded with an accuracy of 75%
- A CCTV image known to contain multiple fault types can be coded with an average IoU of 70%

Introduction

For water companies across the world, CCTV surveys are the primary method of sewer inspection and are vital to the everyday operation of the sewer network. To ensure high quality and uniformity, surveys are annotated according to industry wide standards. In the UK these are specified by the Manual of Sewer Condition Classification or MSCC (WRC plc, 2013), which is comparable to many other international coding standards including PACP in the USA and ISYBAU in Germany. Although previous literature has explored the automated analysis of CCTV footage, very few investigations have annotated images according to an industry standard coding (Haurum & Moeslund, 2020). This is a requirement for widespread acceptance and application in the water industry. Ideally, new AI techniques will need to demonstrate the ability to code surveys to the same standards required of a human technician.

Previous work has focused on (binary) detection of individual fault types; see Haurum & Moeslund (2020) for a review. Only a handful of papers have investigated the classification of fault types as well. Meijer et al. (2019) applied a Convolutional Neural Network (CNN) to over 2.2 million images (~1% containing faults). This identified 12 of the most common fault types and aggregated the results to provide a prediction of pipe condition. Similarly, Li et al. (2019) applied a CNN to identify 6 main fault types, grouping all other faults into an ‘ELSE’ category. Both above methods used oversampling to ameliorate the difficulties arising from imbalanced fault classes, and showed promising results with Li et al. (2019) achieving a peak classification accuracy of 83%.

Unlike the previous work, where only a handful of fault classes are identified, the work presented here aims to annotate 102 specific fault codes in CCTV images. This is an extremely ambitious step building on the success of previous autonomous fault detection (Myrans, et al., 2018) and classification (Myrans, et al., 2019) methods.

Methodology

The proposed method for automated fault coding adapts and extends the original autonomous fault detection methodology (Myrans, et al., 2018), to identify the correct code for an image known to contain a fault. The coding method uses the same pre-processing and feature extraction stages of the existing detection method. Pre-processing simplifies an image, reducing it to a uniform resolution and converting from colour to greyscale. Feature extraction further simplifies the image by calculating a pre-defined feature descriptor for the processed image. This is commonly a GIST descriptor although HOG descriptors have been shown to be similarly effective. Unlike previous work, identification of a code is performed by a bank of ‘one vs rest’ (OVR) classifiers (one OVR classifier for each fault type). Each ‘one vs rest’ classifier comprises an ensemble of random forest classifiers (one for each code). Each random forest estimates the probability of an image containing a specific fault code over that of any other relevant codes. By applying the correct ‘one vs rest’ classifier to the known fault type, the most probable fault code can be assigned. When multiple faults may be present, multi-label analysis is used, so that all codes over a pre-determined threshold assigned. This process is outlined in Figure 1, which shows the processing for coding root intrusion faults.

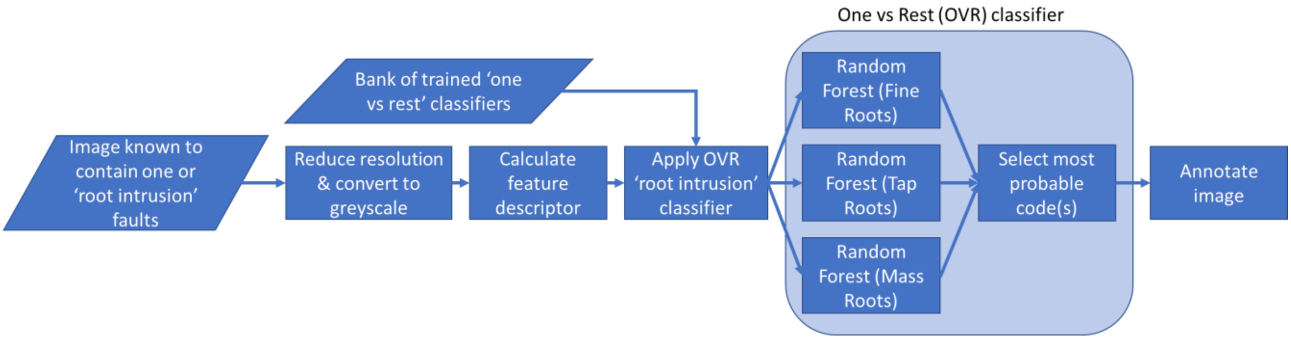

Figure 1. Flowchart outlining the application of fault coding for an image known to contain a 'root intrusion' fault. Note that if multiple fault types were present, an OVR classifier would be applied for each known fault type.

It must be recognised that this method can only be applied if the general type (see Table 1. for a list) of a fault is known or has been previously predicted. As such, this tool is designed to build upon any tool capable of automatically identifying fault types within an image. Given the shared pre-processing and feature extraction stages, the previous detection and classification methods developed by Myrans et al. would prove to be an efficient choice (having negligible impact on processing times).

Results & Discussion

The method has been evaluated on a dataset provided by South West Water, which contains 30,000 images and over 37, 000 labels of faults (as some images contain more than one fault). Note that all faults, features and observations from a survey have been referred to as faults for the sake of brevity. The fault coding methodology was applied to these images for each fault type independently using 25-fold cross validation or 'leave one out' cross validation where fewer than 25 images were available. Doing so evaluated every image in the dataset, whilst avoiding contamination of training and test sets. HOG descriptors (Dalal & Triggs, 2005) were used for this preliminary experiment and each Random Forest contained 10 trees.

Table 1. Results of the preliminary application of the automated fault coding method, where each fault type was evaluated independently. '# Codes' refers to the number of fault codes attributed to a fault type, '# Images' refers to the number of available images for a given fault type and 'Acc. (%)' refers to the percentage accuracy of the codes assigned.

Type	# Codes	# Images	Acc. (%)	Type	# Codes	# Images	Acc. (%)
Connection	2	1264	**98.6**	**Infiltration**	4	379	**78.8**
Loss of Vision	4	519	**94.5**	**Root Intrusions**	3	3280	**77.2**
Shape Change	2	18	**94.4**	**Defective Junction**	5	213	**72.3**
Sealing Ring	2	26	**94.2**	**Settled Deposits**	4	1902	**66.2**
Displaced Joint	3	1036	**91.7**	**Lining Defect**	5	212	**65.4**
Junction	2	2985	**89.5**	**Defective Connection**	9	431	**64.6**
Ingress of Soil	2	2985	**83.3**	**Line**	4	2334	**60.6**
Point Repair	3	551	**82.6**	**Material Change**	15	259	**59.0**
Attached Deposits	4	3113	**82.2**	**Open Joint**	2	195	**51.3**
Surface Damage	9	320	**82.2**	**Lining Change**	2	12	**41.7**
Fracture	5	10143	**80.1**	**Obstacles**	6	47	**24.5**
Crack	5	5617	**79.2**	**Total / Average**	**102**	**37841**	**74.5**

On average (across all fault types) the method achieved a coding accuracy of 75%. However, the accuracy for individual fault types varies substantially. Where the method was applied to over 100 examples it performed well, best on 'Connection' (98.6%), 'Loss of Vision' (94.5%) and 'Displaced joint' (91.7%) faults, and worst on 'Open Joint' (51.3%), 'Material Change' (59.0%) and 'Line' (60.6%) faults. Samples with fewer than 100 examples have been evaluated too (as per previous work) but this is deemed too few to draw a reliable conclusion.

In general, the results obtained are unsurprising. Connections and Junctions are well defined pipe features, with only a few available fault codes. Similarly, images attributed with loss of vision annotations are very distinct from all other types of observation. Conversely, open joint and line deviation codes could be considered trickier to assign. Open joints can be hard to quantify for a surveyor without using pan/tilt functionality, as the camera angle often distorts the view, making the severity of the fault much harder to discern. Equivalently, line deviations are often subtle with most changes in direction being gradual, making them especially tricky to discern from a single image.

As it is common for multiple sewer faults to be present in any given image, the methodology was also applied to the entire dataset of 30,000 images in a multi-label manner. This application used 50-fold cross validation over the entire shuffled dataset without stratifying fault types/codes. The method achieved an average intersection over union (IoU) score of 70%. IoU is a common measure for the accuracy of a multi-label classifier, identifying the similarity between the true and predicted set of labels. In this case it is used as a measure of the method's multi-label accuracy when identifying the similarity between the method's predicted codes and those assigned by the surveyor (considered the ground truth).

Conclusions & Future Work

To conclude, this method of identifying fault codes for the automatic annotation of CCTV sewer surveys shows promising results. Over all 102 fault codes the method achieved an average accuracy of 75% and a multi-label intersection over union (IoU) of 70%. This ability to provide fault codes according to UK industry standards, makes the method much more appealing to practicing surveyors and brings the technology another step closer to industrial application.

The work presented here only demonstrates preliminary investigations into the full coding of CCTV sewer surveys. Future work will seek to improve the current method by using synthetic data and oversampling to provide additional examples of underrepresented codes. As per the previous fault detection and classification methods, temporal smoothing is also a logical next step for improving the method's accuracy, correcting predicted fault codes based on the predictions from neighbouring frames. To reach the full level of detail prescribed by MSCC5 (WRC plc, 2013) additional annotations need to be provided alongside each code, including clock references, sizes and percentages. This will require further research and will likely require the use of additional machine learning tools. Finally, it will be important to apply the full automated sewer analysis technology in full (detection, classification and coding) to gauge its current effectiveness and the current potential for application within the surveying industry.

References

Dalal, N. & Triggs, B., 2005. Histogram of oriented gradients for human detection. *Computer Vision and Pattern Recognition,* pp. 886-893.

Haurum, J. & Moeslund, T., 2020. A survey on Image-Based Automation of CCTV and SSET Sewer Inspections. *Automation in Construction,* Volume 111, p. 103061.

Li, D., Cong, A. & Guo, S., 2019. Sewer damage detection from imbalanced CCTV inspection data using deep convolutional networks. *Automation in Construction,* Volume 101, pp. 199-208.

Meijer, D., Scholten, L., Clemens, F. & Knobbe, A., 2019. A defect classification methodology for sewer image sets with convolutional neural networks. *Automation in Construction,* pp. 281-298.

Myrans, J., Everson, R. & Kapelan, Z., 2019. Automated detection of fault types in CCTV sewer surveys. *Journal of Hydroinformatics,* pp. 153-163.

Myrans, J., Everson, R. & Z., K., 2018. Automated detection of faults in sewers using CCTV image sequences. *Automation in Constrauction,* Volume 95, pp. 64-71.

WRC plc, 2013. *Manual of Sewer Condition Classification.* 5th ed. Swindon: WRC Publications.